

5-2017

Assessing the importance of the root mean square (RMS) value of different waveforms to determine the strength of a dielectrophoresis trapping force

Jordan Gilmore
Clemson University

Monsur Islam
Clemson University

Josie Duncan
Clemson University

Rucha Nato
Clemson University

Rodrigo Martinez-Duarte
Clemson University, rodrigm@clemson.edu

Follow this and additional works at: https://tigerprints.clemson.edu/mecheng_pubs

 Part of the [Mechanical Engineering Commons](#)

Recommended Citation

Please use the publisher's recommended citation. <http://onlinelibrary.wiley.com/doi/10.1002/elps.201600551/abstract>

This Article is brought to you for free and open access by the Mechanical Engineering at TigerPrints. It has been accepted for inclusion in Publications by an authorized administrator of TigerPrints. For more information, please contact kokeefe@clemson.edu.

SHORT COMMUNICATION

Assessing the Importance of the Root Mean Square (RMS) Value of Different Waveforms to Determine the Strength of a Dielectrophoresis Trapping Force

Jordon Gilmore*, Monsur Islam*, Josie Duncan, Rucha Natu, and Rodrigo Martinez-Duarte#

Multiscale Manufacturing Laboratory, Department of Mechanical Engineering, Clemson University, Clemson SC 29634

* Both authors contributed equally to this work

Corresponding author: rodrigm@clemson.edu

Different fabrication technologies are now available to implement the electric field gradient required to induce a dielectrophoretic (DEP) force across a sample of interest [1]. However, the optimization of the polarizing waveform is still an understudied topic. Here we present a methodical comparison between the use of sinusoidal, square and triangular signals to polarize a DEP array for particle trapping. Limited work has been done in this area, and always in function of the application being developed [2]–[4]. It is known that the strength of the DEP force is proportional to the root mean square (RMS) value of the polarizing signal [5]. The RMS amplitude of sinusoidal, square and triangular signals is $\frac{A}{\sqrt{2}}$, A , and $\frac{A}{\sqrt{3}}$ respectively, where A is the peak amplitude of the signal. Some authors reported that time-based differences, *i.e.* shape, amplitude, or frequency, in AC (alternating current) signals contribute to changes in DEP behavior [2]–[4]. We postulate that these changes are the result of the time-averaged RMS voltage, which normalizes the effect of time on changing AC signals. We show that the trapping of particles using positive DEP (pDEP) is approximately the same regardless of the shape of the polarizing signal; as long as the waveforms feature an equivalent RMS voltage magnitude.

We characterized the trapping characteristics of 1.1 ± 0.12 μm -diameter polystyrene particles (yellow-green fluorescent, Magsphere Inc.) on an array of 3D carbon post electrodes (100 μm height by 50 μm diameter). A microchannel made with double-sided pressure-sensitive adhesive contained the electrode array. The reader is referred to our previous publications to consult the fabrication details of these flow-through carbon-electrode DEP devices [6]–[9]. Particles were suspended in distilled water at a concentration of $10^7/\text{ml}$. We characterized the differences in particle trapping when using waveforms with a given frequency and either equivalent peak-to-peak voltages (V_{pp}), equivalent wave energy (E_x) or equivalent RMS voltage (V_{RMS}). The frequency range of 5 kHz – 50 kHz was used for this work due to previous work showing pDEP for 1.1 μm polystyrene beads [10]. The Clausius-Mossotti factor for these experiments decreased by 0.05 across this frequency range.

The experimental protocol featured three stages: trap, wash and release. They consisted of 1) flowing 58 μl of the particle suspension through an electrode array polarized with a specific signal; 2) flowing 60 μl of clean water to wash any trapped particles; and 3) recording the release of particles upon turning the polarizing signal off. The flow rate through the channel was 20 $\mu\text{l}/\text{min}$ and held constant using a syringe pump. The cross-section of the channel was 127 μm -high by 1.75 mm-wide and the gap between carbon electrodes was 58 μm . To characterize the elution pattern for each experiment case, we defined a region of interest (ROI) immediately after the last column of electrodes in the array. We then captured sequential images (600 frames at 10 frames/s) of this region right before and after turning the field off. Depolarization of the electrodes occurred in frame 100. We used ImageJ to obtain the average fluorescence intensity in the ROI throughout particle elution for all experiments. Frames 1-100 recorded the region of interest before turning the field off. Due to the washing step, the fluorescence intensity of

these frames was relatively constant and reflected the fluorescence from the channel filled with water. Hence, we normalized the fluorescence intensity in frames 101-300 to the intensity obtained before turning the field off. Such analysis allowed for the comparison of the strength of particle trapping using different conditions. We report our results below in arbitrary units (a.u.) of fluorescence. The bulk of the particles eluted during the first 300 frames after turning the field off. Thus, we did not analyze frames 301-600.

The focus of this work was on characterizing the difference in particle trapping depending on the waveform. We started by studying different waveforms but with the same frequency and peak-to-peak voltage (V_{pp}). Square, sinusoidal and triangular signals with amplitude of either 15 or 5 V_{pp} were obtained directly from the function generator. The principal finding from this initial set of experiments was that in all cases, the strongest particle trapping happened when using a square signal (figures 1A and 1C). This is in agreement with other authors [3],[11]–[14]. As expected from the RMS values of the waveforms analyzed here, the use of sinusoidal signals afforded for the second strongest trapping. Triangular waveforms enabled the least trapping. The ratio between the fluorescence levels measured when using different polarizing signals is shown in Figure 1B and 1D for 15 and 5 V_{pp} respectively. For 15 V_{pp} , the ratios square:sinusoidal, square:triangular, and sinusoidal:triangular approximate well to the expected $\sqrt{2}$, $\sqrt{3}$, and $\sqrt{\frac{3}{2}}$. However, this is only at frequencies between 5 and 20 kHz. The relation between the different signals at frequencies outside this range remains inconclusive, due to experimental artifacts and limitations imposed by the particular image acquisition system used here. Below 5 kHz, inconsistent particle trapping and an irregular bead response around the electrodes was observed. At frequencies higher than 20 kHz, the DEP force acting on the beads was weak, leading to diminished trapping. Hence, such results could only include the analysis of a few particles. In the case of 5 V_{pp} , the square:sinusoidal relationship held around the expected value of $\sqrt{2}$ for 5 and 10 kHz, whereas square:triangular and sinusoidal:triangular held at $\sqrt{3}$ and $\sqrt{\frac{3}{2}}$ respectively only at 5 kHz. As in the previous case, the weak DEP force exerted on the particles at these polarizing values resulted in inconclusive results.

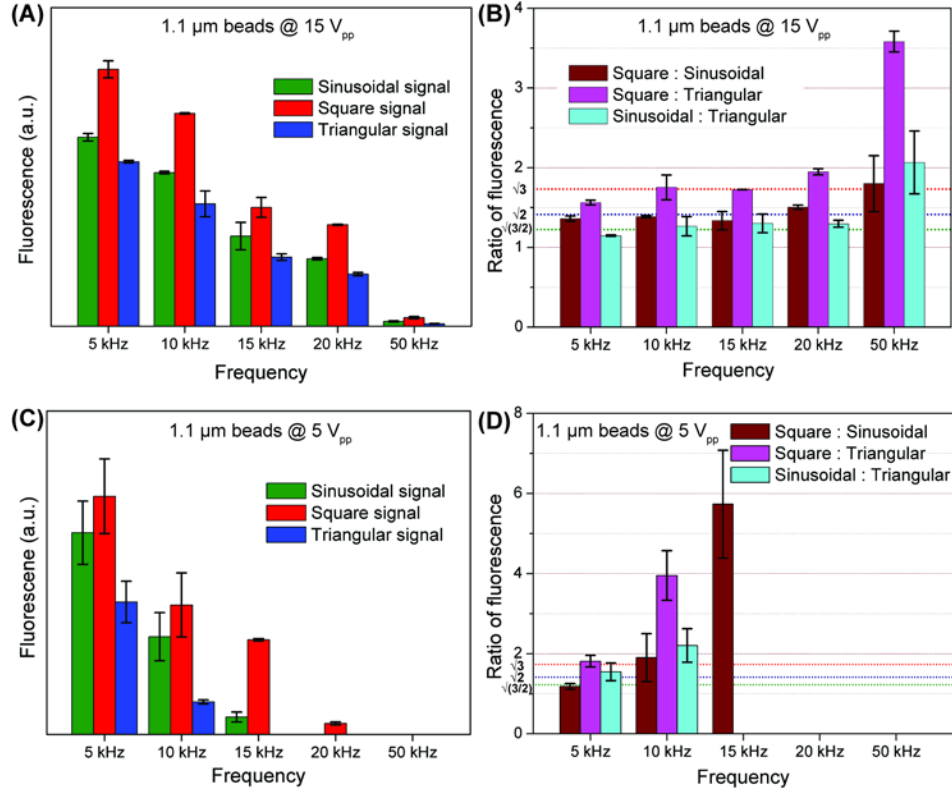


Figure 1: (A and C) Results from particle trapping using square, sinusoidal, and triangular signals with equal V_{pp} . (B and D) Ratio of fluorescence obtained for each of the wave form combinations as calculated from results in figures A and C. The number of samples (N) = 3 for the figure 1A and 1C. Values reported are the mean values from each group of experiments.

The next step in this study was to characterize the trapping behavior depending on the energy delivered to the sample through the electrodes. To calculate the equivalent energy of each waveform, the square signal was first integrated with respect to time over one period. We used the general equation 1 below to obtain the energy value E_x . A_x and $g_x(t)$ corresponded to the peak voltage amplitude V_p and waveform of signal x , which can be square, sinusoidal, or triangular. We first obtained the energy value for a square signal of 5 V_{pp} using a MATLAB script developed in-house (available as supplementary information). This energy value was 7.854 J and was used to calculate the peak amplitude for the sine (7.84 V_{pp}) and triangle (9.98 V_{pp}) waves using the same script. Hence, the different polarizing waveforms used in this set of experiments featured the same frequency and energy, but different peak amplitudes (figure 2A) and RMS values. The RMS value for the square signal was 5 V_{RMS} . Those of sinusoidal and triangular were 5.54 and 5.76 V_{RMS} respectively. Note how the peak voltage and RMS value follow the same hierarchy: triangular, sinusoidal and square.

$$\text{Equation 1} \quad E_x = \int_0^\pi |A_x * g_x(t)|^2 dt$$

The results for particle trapping using these different signals with equivalent energy are presented in figure 2B. The ratios between them are shown in figure 2C. Despite having equivalent energy, the results follow the same trend as those shown in the section above. If signal energy was primarily responsible for particle trapping, the ratio between the different signals would be 1 for any frequency. This is, there will be equivalent trapping for equivalent energy. Instead, the triangular signal (5.76 V_{RMS} and 9.98 V_{pp}) features the strongest trapping at all frequencies, while the square one (5 V_{RMS} , 5 V_{pp}) shows the weakest.

In view of the results obtained above using signals with equal peak to peak voltage and energy, we grew more confident that the RMS value was the main factor to account for DEP trapping.

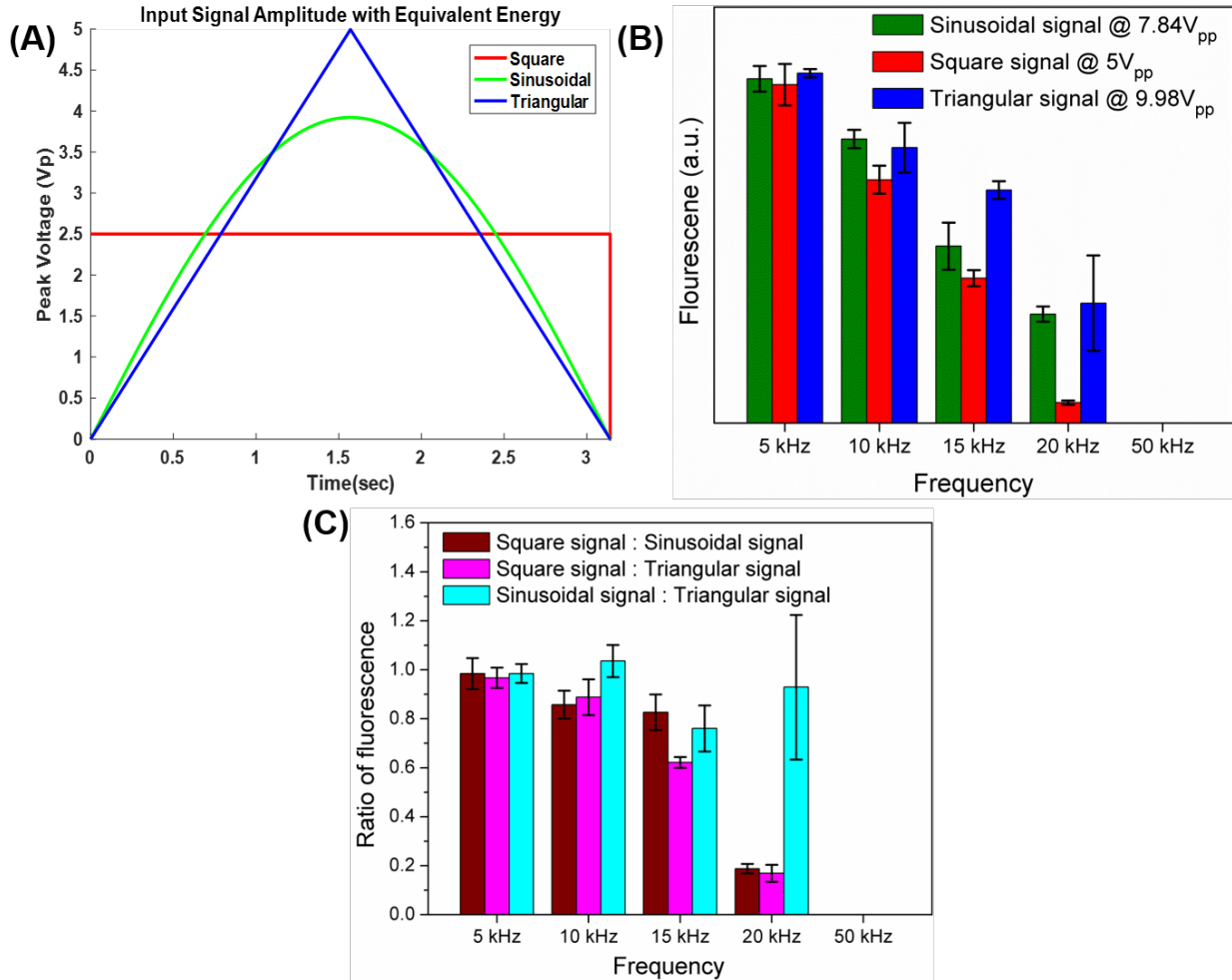


Figure 2: (A) The amplitude of sinusoidal and triangular signals was modulated to feature an energy equivalent to that of the 2.5 V_p, or 5 V_{pp}, square wave. (B) Results from particle trapping using square, sinusoidal, and triangular waveforms of equivalent energy (7.854 J). (C) Ratio of fluorescence for different signal combinations. $N = 3$ for experiments represented in Figure 2B. Values reported are sample means for each frequency tested.

The last step in this work was to characterize trapping when using different waveforms with the same frequency and RMS value of 10 V_{RMS}. Hence, we used a square signal with 10 V_{pp}, a sinusoidal with 14.14 V_{pp} and a triangular one with 17.32 V_{pp}. The results are shown in Figure 3. As before, the trapping decreased with an increase of frequency. However, trapping at all frequencies is similar regardless of the waveform. Such result was also confirmed by assessing the particle concentration around electrodes polarized by the different waveforms with constant V_{RMS}. The fluorescence intensity was monitored over time in a ROI next to the electrodes and is reported in figure 3B. The values of the three curves overlap during initial concentration and stabilize at the same fluorescence intensity.

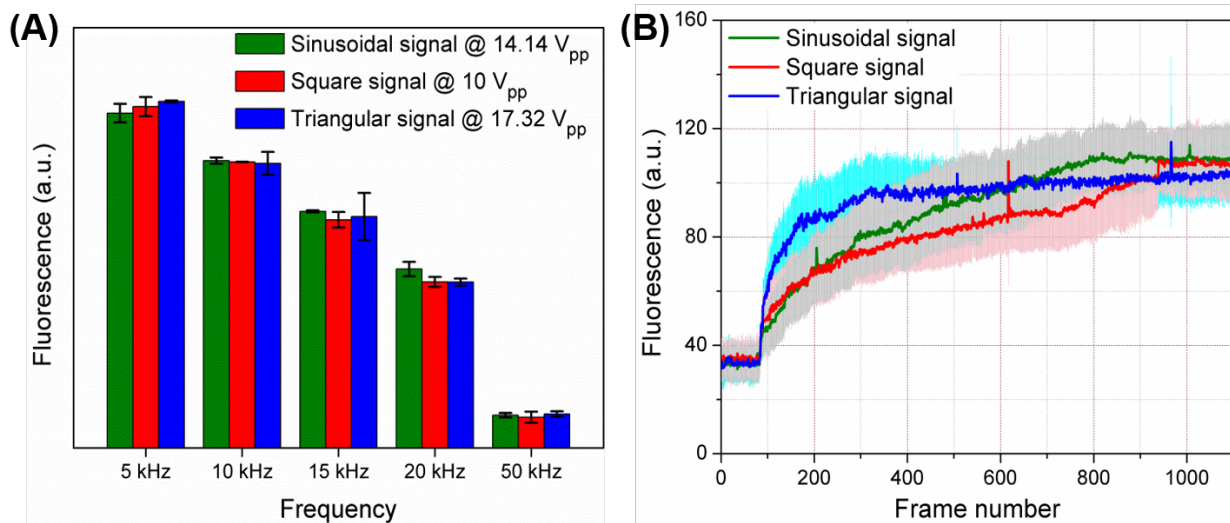


Figure 3: A) Results for particle trapping using waveforms with equivalent $10 V_{RMS}$ but varying V_{pp} . B) Fluorescence intensity obtained by monitoring particle accumulation around electrodes polarized by different signals. Colored curves represent the average value while their shadows represent the range of values obtained for each frame. $N = 3$ for experiments represented in Figure 3A and 3B. Values reported are sample means.

The results from this work demonstrate dependence of the strength of pDEP trapping on the nature of the waveform used to polarize the 3D carbon electrodes. We analyzed multiple waveforms with respect to their peak-to-peak voltage amplitude (V_{pp}), RMS voltage (V_{RMS}), and signal energy (E_x). The conclusion is that RMS voltage is primarily responsible for differences in DEP trapping efficiency with varying signal shape. The use of square signals can alleviate the voltage requirements needed from a signal generator which can translate to less expensive instrumentation to drive DEP devices. For example, the use of a $10 V_{pp}$ amplitude when using a square signal yielded results similar to those obtained when using sinusoidal and triangular signals of higher amplitude, 14.14 and $17.32 V_{pp}$ respectively. Nevertheless, the harmonics that result from square and triangular signals must be taken into account. Some authors reported the harmonics that result from the use of imperfect square signals to be detrimental to DEP trapping efficiency [15]. Others reported such harmonics to enhance the DEP force under specific applications [16],[17]. Nerowski et al further reported on the advantages of increasing the number of harmonics towards using a perfect square signal [18]. Ideally, a fundamental frequency would be selected to avoid detrimental effects from its harmonics. Unfortunately, this will not always be possible due to restrictions such as the nature of the suspending media and the targeted particles. A bandpass filter could be implemented to isolate a specific frequency of interest when using square or triangle waveforms. However, this would defeat the original purpose of simplifying the electronics used to drive the system. For highly specific trapping around a particular fundamental frequency, the sinusoidal signal may remain the best option due to the lack of signal harmonics. This fundamental study was performed with inert beads and the effect of the choice of signal on the viability of biological cells must be further studied to widen the impact of the results presented here. Furthermore, potential cell damage from long exposure times to the different signals must be addressed. Microorganisms are known to tolerate higher membrane loading than mammalian cells and the use of square signals may prove highly beneficial for bacterial processing.

The authors acknowledge Guillermo Contreras Dávila, José Gómez Quiñones and Víctor Pérez for initial experiments and discussion regarding the use of the harmonics of a square signal to improve DEP trapping. JD and RMD acknowledge financial support from Clemson University Creative Inquiry program project #791.

- [1] Martinez-Duarte, R., *Electrophoresis*, 2012, 33, 3110–3132.
- [2] Ouyang, M., Zhang, G., Li, W. J. and Liu, W. K., in *2011 IEEE Intl Conf Robotics and Biomimetics (ROBIO)*, IEEE, 2011, pp. 1397–1402.
- [3] Liang, W., Wang, S., Dong, Z., Lee, G.-B. and Li, W. J., *Micromachines*, 2012, 3, 492–508.
- [4] Biris, A. S., Saini, D., Srirama, P. K., Mazumder, M. K., Sims, R. A., Calle, C. I. and Buhler, C. R., in *2004 IEEE Industry App Conf, 39th IAS Annual Meeting.*, IEEE, 2004, vol. 2, pp. 1283–1286.
- [5] Pethig, R., *Biomicrofluidics*, 2010, 4, 22811.
- [6] Jaramillo, M. D. C., Martínez-Duarte, R., Hüttener, M., Renaud, P., Torrents, E. and Juárez, A., *Biosens. Bioelectron.*, 2013, 43, 297–303.
- [7] Martinez-Duarte, R., Camacho-Alanis, F., Renaud, P. and Ros, A., *Electrophoresis*, 2013, 34, 1113–1122.
- [8] Islam, Monsur, Natu Rucha, Larraga-Martinez Maria Fernanda, M.-D. R., *Biomicrofluidics*, 2016, 10.
- [9] Elitas, M., Martinez-Duarte, R., Dhar, N., McKinney, J. D. and Renaud, P., *Lab Chip*, 2014, 14, 1850–7.
- [10] Yafouz, B., Kadri, N. and Ibrahim, F., *Sensors*, 2014, 14, 6356–6369.
- [11] Reichle, C., Sparbier, K., Müller, T., Schnelle, T., Walden, P. and Fuhr, G., *Electrophoresis*, 2001, 22, 272–282.
- [12] Gimsa, J., Müller, T., Schnelle, T. and Fuhr, G., *Biophys. J.*, 1996, 71, 495–506.
- [13] Muller, T., Pfennig, A., Klein, P., Gradl, G., Jager, M. and Schnelle, T., *IEEE Eng. Med. Biol. Mag.*, 2003, 22, 51–61.
- [14] Contreras Davila, G., Gomez-Quinones, J. I., Perez-Gonzalez, V. H. and Martinez-Duarte, R., *ECS Trans.*, 2016, 72, 105–114.
- [15] Current, W. K., Yuk, K., McConaghy, C., Gascoyne, P. R. C., Schwartz, J. A., Vykoukal, J. V. and Andrews, C., in *Intl Conf. on MEMS, NANO, and Smart Systems, 2005*, IEEE, 2005.
- [16] Shim, H. C., Kwak, Y. K., Han, C.-S. and Kim, S., *Phys. E Low-dimensional Syst. Nanostructures*, 2009, 41, 1137–1142.
- [17] Chu, H., Doh, I. and Cho, Y., *Lab Chip*, 2009, 9, 686–691.
- [18] Nerowski, A., Pötschke, M., Wiesenhütter, U., Nicolai, J., Cikalova, U., Dianat, A., Erbe, A., Opitz, J., Bobeth, M., Baraban, L. and Cuniberti, G., *Langmuir*, 2014, 30, 5655–5661.

Supplementary Information

Matlab script for equivalent energy calculations of square, sine, and triangular waveforms.

```
clear
clc
%%
user_freq = inputdlg('Please enter the frequency of the square wave in Hz');
freq1 = cell2mat(user_freq);
freq2 = str2num(freq1);
t = 0:1/freq2:10;
square_amp = inputdlg('Please enter the amplitude of the square wave in Vpp. ');
amp = cell2mat(square_amp);
A_1 = (str2num(amp)/2);
sq = A_1.*square(t); % Generation of square wave
```

```

sq_fx = @(t) A_1.*square(t); % Generation of square wave but as a function so
that we can do integral
sq_int = integral(sq_fx,0,pi); %Area under square wave curve
[c index] = min(sq);
sq_zero = t(index); % t value where square wave goes from positive to
negative
rect_sq = abs(sq); %Rectified square wave
%%
A_cnt = 1;
while A_cnt < 1000
    A_2 = A_cnt;
    sine = @(t) A_2.*sin(t); % Generation of sine wave
    sine_int = integral(sine,0,pi); %Area under sine wave curve
    diff_sine = abs(sq_int-sine_int);
    if diff_sine > 0.01
        A_cnt = A_cnt + 0.001;
    else
        A_cnt = 1000;
    end
end
B_cnt = 1;
y1= min(0.5,(mod(t,sq_zero)/sq_zero))-0.25; %triangle wave generator
y2= min(0.5,(1-mod(t,sq_zero)/sq_zero))-0.25; %triangle wave generator
while B_cnt < 1000
    A_3 = B_cnt;
    tri = (2*A_3).*(y1+y2); % Triangle signal generator
    tri_int = (0.5)*(pi*A_3); %Area under ramp wave curve, 1/2 bxh
    diff_tri = abs(sq_int-tri_int);
    if diff_tri > 0.01
        B_cnt = B_cnt + 0.001;
    else
        B_cnt = 1000;
    end
end
%%
sine2 = @(t) A_1.*sin(t)
sine2_int = integral(sine2,0,pi);
tri2 = (2*A_1).*(y1+y2);
tri2_int = (0.5)*(pi*A_1);
ratio = [sq_int/sq_int sine2_int/sq_int tri2_int/sq_int];
output = sprintf(' Wave Type - Peak Voltage \n Square - %0.2f \n Sine - %0.2f
\n Triangle - %0.2f \n Ratio = %0.2f:%0.2f:%0.2f for square:sine:triangle
\n',A_1, A_2, A_3,ratio(1),ratio(2),ratio(3));
output_title = sprintf('Equiv. Waves - %0.0f Hz',freq2);
h = msgbox(output,output_title);
figure
[f1,e1] = fplot(sq_fx,[0 pi],'r-');
hold on
[f2,e2] = fplot(sine, [0 pi],'g-');
f3 = plot(f1,e1,'r');
f4 = plot(f2,e2,'g');
plot(t,tri,'b-', 'LineWidth',2);
set([f3 f4], 'LineWidth',2);
limitsx = [0 pi];
xlim(limitsx);
limitsy = [0 max(tri)];
ylim(limitsy);

```



```
legend('Square','Sine','Triangle')
title('Input Signal Amplitude with Equivalent Energy');
xlabel('Time(sec)');
ylabel('Peak Voltage (Vp)');
```